



Development of N -[^{11}C]methylamino 4-hydroxy-2(1*H*)-quinolone derivatives as PET radioligands for the glycine-binding site of NMDA receptors

Takeshi Fuchigami^{a,c}, Terushi Haradahira^b, Noriko Fujimoto^a, Yumiko Nojiri^a, Takahiro Mukai^a, Fumihiko Yamamoto^a, Takashi Okauchi^b, Jun Maeda^b, Kazutoshi Suzuki^b, Tetsuya Suhara^b, Hiroshi Yamaguchi^d, Mikako Ogawa^c, Yasuhiro Magata^{c,d,*}, Minoru Maeda^a

^a Graduate School of Pharmaceutical Sciences, Kyushu University, Higashi-ku, Fukuoka 812-8582, Japan

^b Molecular Imaging Center, National Institute of Radiological Sciences, Inage-ku, Chiba 263-8555, Japan

^c Photon Medical Research Center, Hamamatsu University School of Medicine, Hamamatsu 431-3192, Japan

^d Molecular Imaging Frontier Research Center, Hamamatsu University School of Medicine, Hamamatsu 431-3192, Japan

ARTICLE INFO

Article history:

Received 5 May 2009

Revised 4 June 2009

Accepted 6 June 2009

Available online 13 June 2009

Keywords:

Glycine-binding site

NMDA receptor

4-Hydroxy-2(1*H*)-quinolone

PET

ABSTRACT

In this study, we synthesized and evaluated several amino 4-hydroxy-2(1*H*)-quinolone (4HQ) derivatives as new PET radioligand candidates for the glycine site of the NMDA receptors. Among these ligands, we discovered that 7-chloro-4-hydroxy-3-{3-(4-methylaminobenzyl) phenyl}-2-(1*H*)-quinolone (**12**) and 5-ethyl-7-chloro-4-hydroxy-3-(3-methylaminophenyl)-2(1*H*)-quinolone (**32**) have high affinity for the glycine site (K_i values; 11.7 nM for **12** and 11.8 nM for **32**). In vitro autoradiography experiments indicated that [^{11}C]**12** and [^{11}C]**32** showed high specific binding in the brain slices, which were strongly inhibited by both glycine agonists and antagonists. In vivo brain uptake of these ^{11}C -labeled 4HQs were examined in normal mice. Cerebellum to blood ratio of accumulation, of both [^{11}C]**12** and [^{11}C]**32** at 30 min were 0.058, which were slightly higher than those of cerebellum to blood ratio (0.043 and 0.042, respectively). These results indicated that [^{11}C]**12** and [^{11}C]**32** have poor blood brain barrier permeability. Although the plasma protein-binding ratio of [^{11}C]**32** was much lower than methoxy analogs (71% vs 94–98%, respectively), [^{11}C]**32** still binds with plasma protein strongly. It is conjectured that still acidic moiety and high affinity with plasma protein of [^{11}C]**32** may prevent in vivo brain uptake. In conclusion, [^{11}C]**12** and [^{11}C]**32** are unsuitable for imaging cerebral NMDA receptors.

© 2009 Elsevier Ltd. All rights reserved.

1. Introduction

The *N*-methyl-D-aspartate (NMDA) receptor is known to play a central role in excitatory neurotransmission, such as learning, memory, and synaptic plasticity. Dysfunction of this receptor is thought to be involved in various disorders, including epilepsy, ischemic brain damage, and neurodegenerative disorders, such as Parkinson's and Alzheimer's diseases. The NMDA ion channel has, therefore, been considered to be a prime therapeutic target in the development of useful neuroprotective strategies.^{1–3} Since glycine is an essential co-agonist for NMDA ion channel activation, various classes of glycine-binding site antagonists with anticonvulsant and neuroprotective properties have been developed.^{1,2} On the other hand, it is suggested that impairment in the NMDA receptor function is associated with the pathophysiology of schizophrenia. Consistent with this theory, clinical trials have demonstrated that the enhancement of NMDA receptor function by potentiating the glycine site of the receptor is efficacious in the

treatment of schizophrenia.⁴ Imaging of the glycine site coupled to the NMDA ion channel by positron emission tomography (PET) is, thus, considered useful for obtaining information about the functional mechanism of the NMDA ion channel in the living brain and in the diagnosis of various neurological disorders.

We recently developed the ^{11}C -labeled 4-hydroxy-2(1*H*)-quinolone (4HQ) derivatives, acetyl-[^{11}C]L-703,717 ([^{11}C]**2**)^{5,6} (a prodrug of [^{11}C]L-703,717 ([^{11}C]**1**)^{7–9} and 3-[^{11}C]methoxy-MDL-104,653 (or 4-hydroxy-3-(3-[^{11}C]methoxyphenyl)-2(1*H*)-quinolone) ([^{11}C]**3**),^{10–12} as PET radioligands for the glycine-binding site (Fig. 1). [^{11}C]**2** is a potential radioligand for use in PET investigations of the cerebellar NMDA ion channel and has recently been applied in the first human trial. In human brain, although, [^{11}C]**2** showed the highest accumulation in the cerebellum, the radioactivity concentration was too low to visualize the cerebellar NMDA receptors by PET, which is indicative of poor brain penetration of [^{11}C]**2**.⁶ More recently we developed high affinity ethyl- and iodine-C-5 substituted analogs of [^{11}C]**3** (K_i values were 7.2 and 10.3 nM for **4** and **5**, respectively). Although [^{11}C]**4** and [^{11}C]**5** have moderate lipophilicity, these ligands did not result in any significant increase in brain uptake.¹³ The 4HQs are all acidic with $\text{p}K_a$

* Corresponding author. Tel./fax: +81 53 435 2398.

E-mail address: magata@hama-med.ac.jp (Y. Magata).

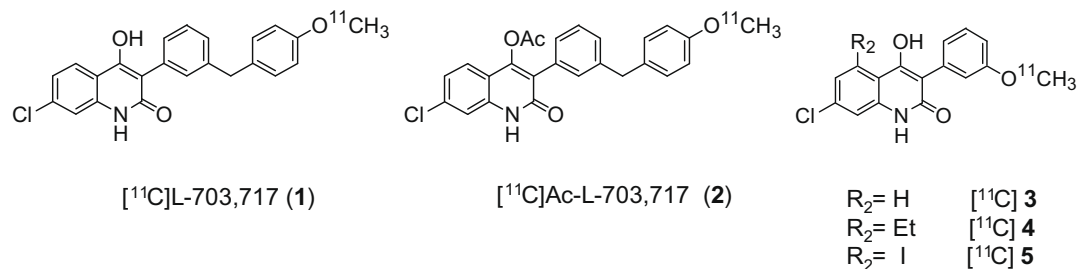


Figure 1. Structure of ^{11}C labeled 4-hydroxy-2-quinolone derivatives.

values of around 5 or below,¹² and more amenable to binding with plasma proteins than non-acidic compounds, resulting in poor blood brain barrier (BBB) penetration. Introduction of basic amino group into 4HQ may increase the pK_a value and reduce unsuitable protein bindings, which could increase the brain uptake. Therefore, in order to develop the glycine/NMDA receptor radioligands with reduced plasma protein binding affinity, we synthesized several amino analogs of 4HQs and examined the in vitro binding properties and in vivo brain uptake characteristics in rodents.

2. Results and discussion

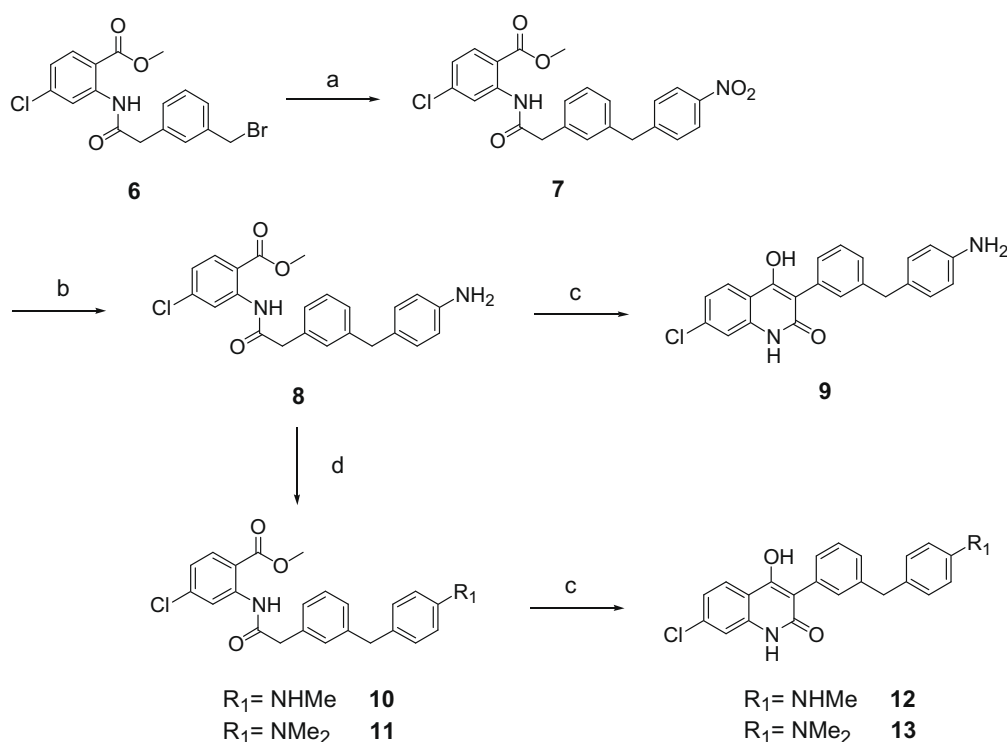
2.1. Chemistry

The L-703,717 (**1**) derivatives substituted at R_1 position with amino groups were prepared as shown in Scheme 1. Palladium-catalyzed Suzuki coupling of **6**¹⁴ with 4-nitrophenylboronic acid formed nitro benzyl derivative **7**, followed by the reduction of the nitro group using TiCl_3 formed amino derivative **8**. Methylation of **8** using methyl iodide gave methylamino derivative **10** and dimethylamino derivative **11**. Cyclization of **8**, **10**, and **11** using potassium carbonate afforded the desired 4HQs **9**, **12**, and **13**, respectively. Compound **19**, which is the L-703,717 (**1**) derivative

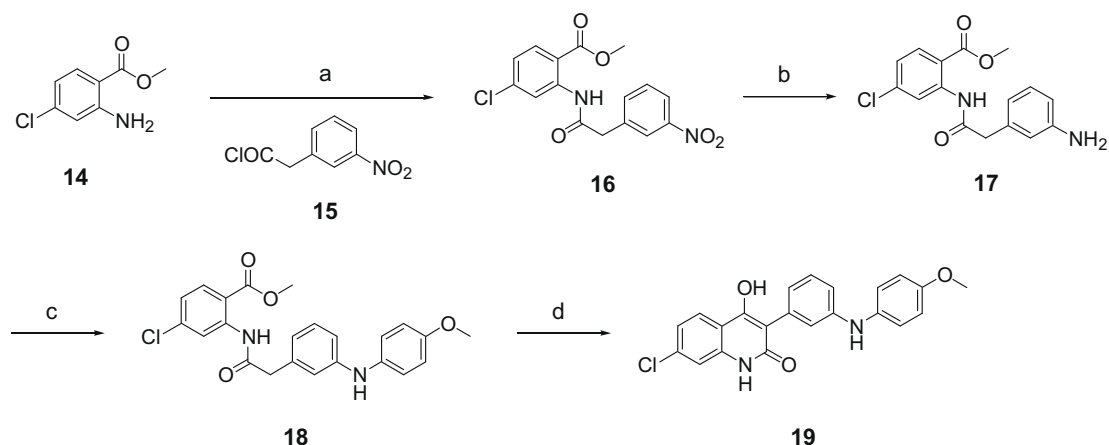
substituted at X-position with amino group, was prepared as shown in Scheme 2. Coupling of methyl anthranilate derivative **14** with acid chloride **15** provided amide derivative **16**, then the reduction of nitro group formed **17**. Copper-catalyzed coupling¹⁵ of **17** with 4-methoxyphenylboronic acid gave compound **18**. Subsequent cyclization of **18** using potassium hexamethyldisilazide afforded the desired compound **19**. The 5-substituted (R_2 -substituted) **3** derivatives were prepared as shown in Scheme 3. Starting with compound **20**,¹⁶ 5-amino derivative **24** was obtained by similar procedure as described above. The 5-methylamino derivative **25** and 5-dimethylamino derivative **27** were synthesized by using the general reductive amination. The compound **4** derivatives with methoxy group at R_3 -position replaced with amino group were prepared as shown in Scheme 4. Starting with compound **28**,¹⁷ the desired 4HQs, **32** and **33**, were obtained by the similar reaction steps as described above.

2.2. In vitro binding assays

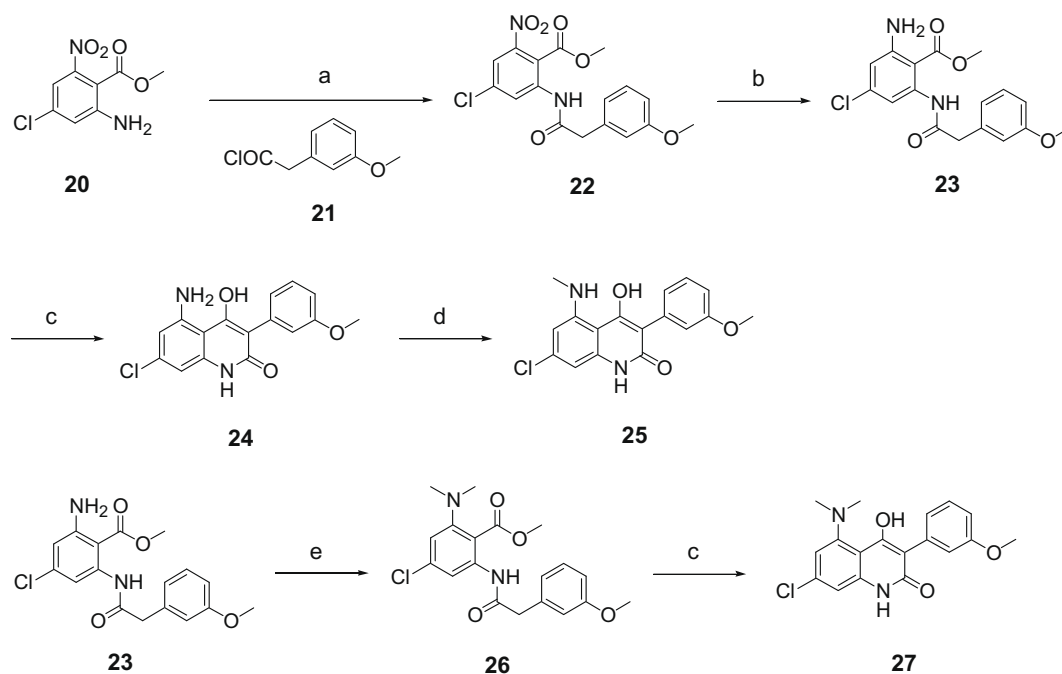
The binding affinities (K_i values) of 4HQs for the glycine-binding sites of the NMDA ion channel were measured by displacement of a typical glycine-site antagonist, [^3H]MDL-105,519, to rat cortical synaptic membranes.¹⁸ The pK_a values of 4-hydroxy group in



Scheme 1. Preparation of 4'-methyl amino derivatives of **1**. Reagents and conditions: (a) $\text{Pd}(\text{Ph}_3)_4$, *p*-nitrophenylboronic acid, Na_2CO_3 , DME, 90 °C, 95%; (b) TiCl_3 , THF, rt, 85%; (c) K_2CO_3 , DMSO, 90 °C, then MeOH, HCl, 77% for **9**, 97% for **12**, 95% for **13**; (d) CH_3I , EtOH, DMF, rt, 23% for **10**, 32% for **11**.



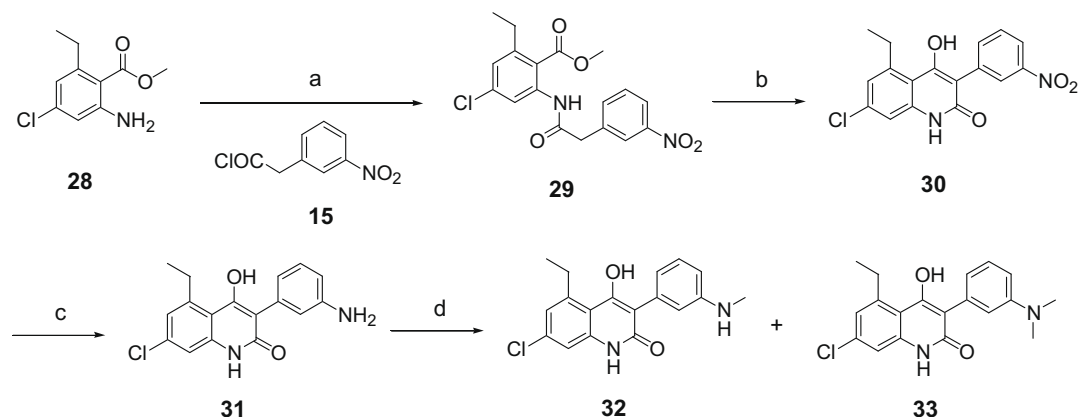
Scheme 2. Preparation of diphenylamino derivative of **1**. Reagent and conditions: (a) $\text{ClCH}_2\text{CH}_2\text{Cl}$, 80°C , 86%; (b) Fe, AcOH, EtOH, 80°C , 97%; (c) $\text{Cu}(\text{OAc})_2$, myristic acid, 2,6-lutidine, 4-methoxyphenylboronic acid, rt, 74%; (d) KHMDS , THF, rt, then TFA, 98%.



Scheme 3. Preparation of 5-amino derivatives of **3**. Reagent and conditions: (a) $\text{ClCH}_2\text{CH}_2\text{Cl}$, 80°C , 95%; (b) Fe, AcOH, EtOH, 80°C , 95%; (c) K_2CO_3 , DMSO, 90°C , 98% for **24**, 98% for **27**; (d) HCHO, NaBH_3CN , MeOH, rt, 71%; (e) HCHO, NaBH_4 , H_2SO_4 , THF, rt, 86%.

4HQs and $\log D_{7.4}$ values of 4HQs were calculated on SPARK on line calculator.¹⁹ As shown in Table 1, replacement of the methoxy group at R_1 -position of **1** with amino groups maintained high receptor affinity. The calculated pK_a value of **12** was comparable with **1** (5.20). Methyl amino derivative **12** had approximately two-fold higher affinity than dimethyl amino derivative **13** (K_i values; 11.7 nM for **12**, 22.2 nM for **13**). Introduction of amino group into X-position of **1** also maintained high binding affinity (K_i value; 23.6 nM for **19**), which was comparable with that of **13**. The calculated pK_a values of **13** and **19** were 5.25 which were slightly higher than that of **12**. These results indicate that the pK_a values of 4-hydroxy group and the binding affinity for the glycine site of 4HQs may not change significantly, when the amino group is introduced at R_1 -position of L-703,717 (**1**). Introduction of NH_2 group into the 5-position (R_2 -position) of **3** ($K_i = 167$ nM) resulted in slightly enhancement of the affinity ($K_i = 119$ nM for **24**). However, 5-methylamino derivative **25** and 5-dimethylamino derivative **27**

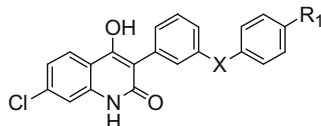
exhibited lower affinity than **24** (K_i values; 715 nM for **25**, 566 nM for **27**). Next, we attempted to introduce the amino groups into R_3 -position of high affinity 5-ethyl derivative **4** ($K_i = 7.20$ nM).¹³ Therefore, methylamino derivative **32** had a high affinity ($K_i = 11.8$ nM), which is comparable with that of **4** ($K_i = 7.20$ nM). On the other hand, dimethylamino derivative **33** had approximately threefold lower affinity ($K_i = 34.3$ nM) relative to **32**. We previously reported that introduction of ethyl group and iodine atom into the 5-position of **3** resulted in a significant enhancement of the affinity (K_i values; 7.2 nM for **4** and 10.3 nM for **5**, respectively) as compared with the parent **3** ($K_i = 167$ nM).¹³ Although binding affinity for glycine site of **4** and **5** were comparable, the pK_a values of **4** and **5** differ greatly. The pK_a value of 5-ethyl derivative **4** is much higher than that of **3**, on the other hand, the pK_a value of 5-iodo derivative **5** is lower than that of **3** (pK_a values; 5.35 for **3**, 5.51 for **4**, and 4.97 for **5**). Introduction of NH_2 or NHMe group into the 5-position of **3** greatly increase pK_a values (pK_a val-



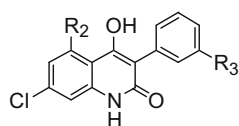
Scheme 4. Preparation of 3'-methyl amino derivatives of **4**. Reagent and conditions: (a) $\text{ClCH}_2\text{CH}_2\text{Cl}$, 80°C , 65%; (b) KMDS , THF, rt, 87%; (c) Fe, AcOH, EtOH, 80°C , 91%; (d) CH_3I , EtOH, DMF, 80°C , 17% for **32**, 8% for **33**.

Table 1

In vitro binding affinity (K_i) of new 4-hydroxy-2-quinolone derivatives for glycine site of the NMDA receptor, experimental octanol/phosphate buffer distribution coefficient ($\log D_{7.4}$), calculated $\log D_{7.4}$, and calculated pK_a of 4-hydroxy group



Compounds	X	R ₁	K_i^a (nM)	$\log D_{7.4}^c$	$\log D_{7.4}^d$	pK_a^e
1	CH ₂	OMe	5.12 ± 0.99^b	3.47	3.84	5.20
12	CH ₂	NHMe	11.7 ± 1.41	3.00	3.08	5.20
13	CH ₂	NMe ₂	22.2 ± 3.62		3.53	5.25
19	NH	OMe	23.6 ± 9.89		2.63	5.25



	R ₂	R ₃	K_i^a (nM)	$\log D_{7.4}^c$	pK_a^e
3	H	OMe	167 ± 23.0^b	1.75	5.35
4	Et	OMe	7.20 ± 1.56^b	2.78	5.51
5	I	OMe	10.3 ± 1.30^b	2.46	4.97
24	NH ₂	OMe	119 ± 456	2.09	5.67
25	NHMe	OMe	715 ± 206	2.35	5.67
27	NMe ₂	OMe	566 ± 197	2.84	5.48
32	Et	NHMe	11.8 ± 3.32	1.92	5.59
33	Et	NMe ₂	34.3 ± 12.9	2.60	5.59

^a The K_i values were obtained by the method in Ref. 18. Each value (mean \pm SD) was determined three times with triplicate using rat cortical membrane homogenates in Tris-HCl buffer.

^b The K_i values have been reported in our previous studies from Ref. 13.

^c The partition coefficient between *n*-octanol and sodium phosphate buffer at pH 7.4 ($\log D_{7.4}$) was determined by conventional shake-flask method ($n = 3$).

^d The $\log D_{7.4}$ values of 4HQs were calculated on SPARK on line calculator.¹⁹

^e The pK_a values of 4-hydroxy group in 4HQs were calculated on SPARK.¹⁹

ues; 5.67 for **24** and **25**, 5.35 for **3**). However binding affinity for the glycine site of these ligands was quite different from each other (K_i values; 119 nM for **24**, 715 nM for **25**). Introduction of the amino groups into R₃-position of **4** slightly increase pK_a values (pK_a values; 5.59 for **32** and **33**). However binding affinity for the glycine site of **33** was threefold lower than that of **32**. The experimental results indicated that the binding affinity of **3** derivatives for the glycine site may have no correlation with calculated pK_a values of 4-hydroxy group in 4HQs. Since **12** and **32** had the highest binding

affinity for the glycine site of the NMDA receptor among the amino derivatives newly synthesized in this study, we chose these ligands to carry out further biological evaluations on the corresponding C-11 labeled probes.

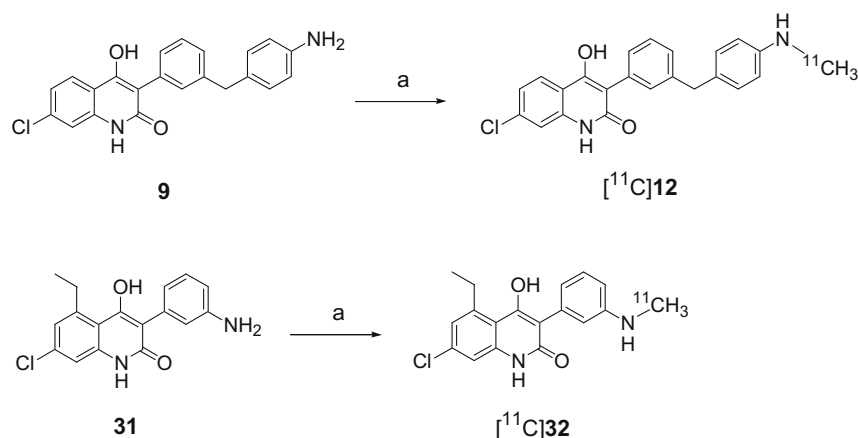
2.3. Radiochemistry

To obtain [¹¹C]**12** and [¹¹C]**32**, the corresponding amino precursors, **9** and **31**, were reacted with [¹¹C]CH₃OTf in acetone at 60°C for 1.5 min (Scheme 5). The resulting C-11 labeled crude products were purified by HPLC. The desired products were obtained in 30 min; and the specific activities at the end of synthesis were 47 GBq/ μmol for [¹¹C]**12** and 63 GBq/ μmol for [¹¹C]**32**, respectively. The radiochemical purities were >98% for both ligands, and the radiochemical yields were 8% for [¹¹C]**12** and 27% for [¹¹C]**32** (decay-corrected).

2.4. In vitro autoradiography

In vitro regional distributions of [¹¹C]**12** and [¹¹C]**32** on the rat brain sections were evaluated by a method similar to that in the literature.²⁰ The results are summarized in Figures 2 and 3. As shown, the autoradiogram in Figure 2, both [¹¹C]**12** and [¹¹C]**32** showed the highest accumulation in the hippocampus, followed by the cerebral cortex, thalamus, striatum, and lowest uptake in the cerebellum (Fig. 2A and C). Nonspecific binding was determined in the presence of corresponding nonradioactive 4HQ (10 μM), which resulted in a significantly lower radioactivity of [¹¹C]**12** and [¹¹C]**32** in the whole brain compared with total binding (Fig. 2B and D). These results are consistent with the brain distributions of other high-affinity glycine-site antagonists.^{21,22} The specific bindings of [¹¹C]**12** and [¹¹C]**32** on the slices were 30% (cerebellum) to 70% (hippocampus) and 75% (cerebellum) to 89% (hippocampus), respectively. Although, both ligands showed high specific bindings in forebrain regions (cerebral cortex, hippocampus), the specific binding ratio of [¹¹C]**12** was higher than that of [¹¹C]**32** in all brain regions (Fig. 2E and F).

In order to investigate the specificity of [¹¹C]**12** and [¹¹C]**32** binding to the glycine site of the NMDA ion channel, we carried out in vitro inhibition studies on rat hippocampal region using glycine-site agonists (glycine and D-serine) and antagonists [L -703,717 (**1**); methoxy-MDL-104,653 (**3**), MDL-105,519], with the results being summarized in Figure 3A (agonists) and B (antagonists). The corresponding methoxy derivatives [¹¹C]**1** and [¹¹C]**4** were also investigated for comparison of binding characters with amino derivatives. The in vitro total bindings of [¹¹C]**12** were



Scheme 5. Radiosynthesis of [^{11}C]12 and [^{11}C]32. Reagent and conditions: (a) [^{11}C]CH $_3$ OTf, acetone, 60 °C, 1.5 min, 8% for [^{11}C]12, 27% for [^{11}C]32 (decay-corrected).

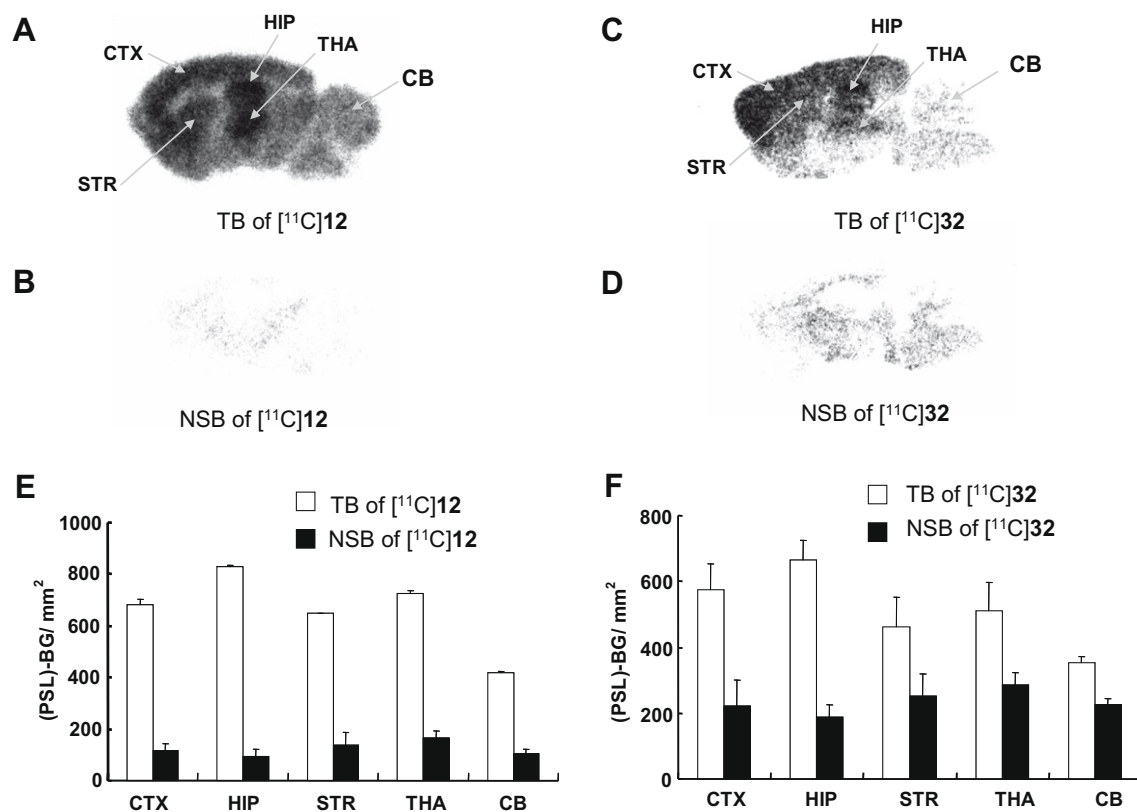


Figure 2. Autoradiogram of in vitro total binding of [^{11}C]12 (A), nonspecific binding of [^{11}C]12 (B), total binding of [^{11}C]32 (C), and nonspecific binding of [^{11}C]32 (D) to rat brain sagittal sections. The quantified values of [^{11}C]12 (E) and [^{11}C]32 (F) in frontal cortex (CTX), hippocampus (HIP), striatum (STR), thalamus (THA), and cerebellum (CB) are expressed as (PSL)-BG/mm 2 (mean \pm SD, n = 4–6). TB, total binding; NSB, nonspecific binding determined in the presence of corresponding nonradioactive 4HQ (10 μM).

strongly inhibited by both glycine-site agonists (46–53%) and antagonists (58–93%), respectively. The bindings of [^{11}C]32 were also inhibited by both agonists (59–66%) and antagonists (64–70%). The inhibition characteristics of ^{11}C labeled amino derivatives 12 and 32 were similar to corresponding methoxy derivatives 1 and 4 (Fig. 3A and B).

Recently, we reported that the binding characters of 4HQs varied according to the substituent groups. The [^{11}C]1 and 5-ethyl analog [^{11}C]4 showed higher in vitro binding in the forebrain regions than in the cerebellum, in which the binding was strongly inhibited by both glycine-site agonists and antagonists. In contrast, [^{11}C]3 and 5-iodo analog [^{11}C]5 showed a homogeneous in vitro

binding throughout the brain which was inhibited by antagonists alone.^{10,13} Previous experimental data, including mutational analysis, support the evidence that glycine-site agonists and antagonists bind to overlapping but different sites on the NMDA ion channel.^{23,24} The existence of multiple glycine agonist domains has also been reported on the NMDA ion channel.²⁵ Thus, it is considered that two binding sites for [^{11}C]4HQs on the NMDA ion channel may be existed, the agonist-sensitive and agonist-insensitive (or antagonist-preferring) sites as described in our previous study.¹³ It is suggested that the agonist-sensitive sites located on the functional NMDA ion channel are formed by the combination of heteromeric NR1 and NR2 subunits. In contrast, the agonist-insensitive

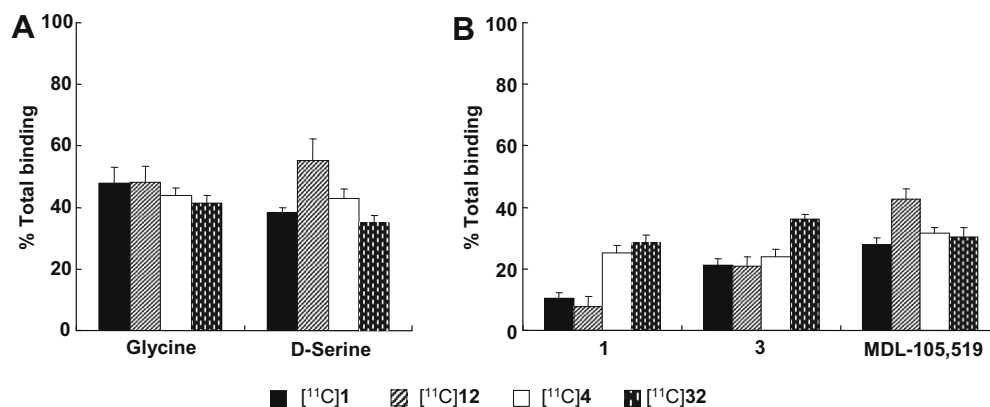


Figure 3. Effects of NMDA agonists (A) and antagonists (B) on in vitro total [^{11}C]4HQ bindings to hippocampus. The PSL data in the presence of drugs were converted to the percentage of control PSL data in the absence of drugs (mean \pm SD, $n = 4$ –6).

sites may exit on homomeric NR1 receptors or desensitized or inactivated NMDA ion channel.²⁶ In fact, the accumulation of [^{11}C] 4HQs in the brain tissue tended to be inhibited by antagonists stronger than agonists (Fig. 3). These experiments indicate that most binding site of [^{11}C]12 and [^{11}C] 32 may overlap with the glycine antagonist binding site. In these studies, [^{11}C]12 and [^{11}C]32 showed high specific binding in the forebrain regions than cerebellum, in which the binding on the latter area was strongly inhibited by both glycine-agonists and antagonists. These results strongly suggest that 4HQs, which have bulky 3-benzyl phenyl group in 3-position, such as **1** and **12**, or ethyl group in 5-position, such as **4** and **32**, demonstrate high specific binding for the functional heteromeric NR1 and NR2 subunits.

The in vitro binding experiments demonstrate that [^{11}C]12 and [^{11}C]32 are useful as PET imaging agents for the functional NMDA receptor. As shown in Table 1, the experimental log $D_{7,4}$ value of **12** and **32** were well correlated with calculated one (3.00 vs 3.08 for compound **12** and 1.92 vs 2.16 for compound **32**, respectively). The lipophilicity of these ligands are in the optimal range (1.0–3.0) for compounds expected to penetrate the BBB.²⁷ Thus, we attempted further in vivo experiments on these radioligands. We previously demonstrated that 4HQs are selective ligands for the glycine site of the NMDA receptor.¹³

2.5. In vivo pharmacology

The biodistribution studies of [^{11}C]1, [^{11}C]4, [^{11}C]12, and [^{11}C]32 were performed by using normal mice and the results were shown in Table 2. All of these ligands exhibited very high blood radioactivity level. The radioactivity of 5-ethyl substituted analogs ([^{11}C]4 and [^{11}C]32) at 1 min were 20.91–29.16% of injected dose per gram of tissue (% dose/g), which were much higher than those of L-703,717 analogs ([^{11}C]1 and [^{11}C]12; 8.37–13.08% dose/g). The radioactivity concentration of [^{11}C] 4HQs in blood were still high level (9.08–10.66% dose/g for 5-ethyl analog and 3.58–3.93% dose/g for L-703,717 analogs) at 30 min. The brain uptake of [^{11}C]12 at 1 min after intravenous injection was 0.53% dose/g in the cerebellum, which was higher than cerebral uptake (0.40% dose/g). After 30 min, the uptake of [^{11}C]12 in the cerebrum and cerebellum were 0.17% and 0.23% dose/g, respectively. The brain to blood ratios of [^{11}C]12 at 1 min and 30 min were 0.031–0.037 and 0.043–0.058, respectively. These results indicate that [^{11}C]12 has poor BBB permeability. The brain uptake of [^{11}C]32 at 1 min after intravenous injection was 0.87% dose/g in the cerebellum, which was much higher than the cerebral uptake (0.47% dose/g). At 30 min, the uptake of [^{11}C]32 in the cerebrum and cerebellum were 0.36% and 0.53% dose/g, respectively. The brain to blood ra-

Table 2
Brain and blood uptake of [^{11}C]4HQs in mice at 1 min and 30 min after injection

	Region	1 min		30 min		30 min Blocking ^a	
		% Dose/g ^b	Tissue/blood ^b	% Dose/g ^b	Tissue/blood ^b	% Dose/g ^b	Tissue/blood ^b
[^{11}C]1	Blood	8.37 \pm 0.60 ^d		3.46 \pm 0.53			
	Cerebrum	0.32 \pm 0.03 ^d	0.038 \pm 0.004	0.20 \pm 0.01	0.051 \pm 0.004		
	Cerebellum	0.36 \pm 0.05 ^d	0.043 \pm 0.005	0.24 \pm 0.05	0.068 \pm 0.007		
[^{11}C]12	Blood	13.08 \pm 0.76		3.93 \pm 0.25			
	Cerebrum	0.40 \pm 0.07	0.031 \pm 0.007	0.17 \pm 0.01	0.043 \pm 0.003		
	Cerebellum	0.48 \pm 0.10	0.037 \pm 0.006	0.23 \pm 0.02	0.058 \pm 0.004		
[^{11}C]4	Blood	29.16 \pm 6.03		10.66 \pm 1.36			
	Cerebrum	0.50 \pm 0.11	0.018 \pm 0.006	0.32 \pm 0.03	0.030 \pm 0.003		
	Cerebellum	0.72 \pm 0.09	0.026 \pm 0.007	0.44 \pm 0.05	0.042 \pm 0.008		
[^{11}C]32	Blood	20.91 \pm 2.34		9.08 \pm 0.70		7.77 \pm 0.72	
	Cerebrum	0.47 \pm 0.10	0.022 \pm 0.003	0.38 \pm 0.06	0.042 \pm 0.008	0.34 \pm 0.05	0.044 \pm 0.004
	Cerebellum	0.87 \pm 0.03	0.042 \pm 0.011	0.53 \pm 0.03 ^{c,e}	0.058 \pm 0.006	0.34 \pm 0.04 ^f	0.044 \pm 0.002 ^f

^a Non-radioactive **32** was co-administrated with [^{11}C]32.

^b Mean \pm SD ($n = 3$).

^c Mean \pm SD ($n = 5$).

^d Data from Ref. 13.

^e $P < 0.01$ in comparison to the cerebrum (Mann–Whitney U -test).

^f $P < 0.05$ in comparison to the control group (Mann–Whitney U -test).

tios of [^{11}C]**32** at 1 min and 30 min were 0.022–0.042 and 0.038–0.053, respectively. Considering these results, [^{11}C]**32** may also have low BBB permeability. The uptake of [^{11}C] 4HQs in the cerebellum tend to be slightly higher than in the cerebrum. These in vivo results are inconsistent with in vitro brain distribution of radioligands. Previously, we demonstrated that the agonist-sensitive [^{11}C]**1** and its pro-drug [^{11}C]**2** show high in vivo specific binding in the cerebellum.^{5,9} The different brain uptake of [^{11}C]**1** between in vitro and in vivo condition may be due to the regional brain differences in endogenous agonist levels. It is known that endogenous glycine agonists, such as glycine and D-serine, exist in μM quantities in the brain.¹ Glycine is high in the brainstem/spinal cord but low in the cerebellum/forebrains. On the contrary, D-serine is high in the forebrains but is undetectable in the cerebellum.²⁸ Thus, it is considered that the existence of endogenous glycine agonists in cerebellum is lower than in the cerebrum under in vivo condition. In fact, we demonstrated a greatly diminished cerebellar localization of [^{11}C]**1** in mutant mice lacking the D-amino acid oxidase (DAO); wherein, the D-serine content in the cerebellum is drastically increased from a nondetectable level in normal mice.²⁹ Therefore, it is suggested that agonist-sensitive ligands, [^{11}C]**12** and [^{11}C]**32**, showed high cerebellar accumulation for a similar reason.

Although the uptake of ^{11}C amino derivatives of 4HQs were low level, the radioactivity of [^{11}C]**32** in brain and blood are much higher than that of [^{11}C]**12** as shown in Table 2. In addition, the calculated pK_a value of [^{11}C]**32** was much higher than that of [^{11}C]**12** (5.59 and 5.20, respectively). Therefore we performed further experiments of [^{11}C]**32**. Metabolisms of [^{11}C]**32** in mouse brain and blood were analyzed by radio-TLC of brain homogenates obtained at 30 min post-injection; and 70% and 93%, respectively, of the parent compounds remained unchanged (data not shown). The in vivo stability of [^{11}C]**32** is comparable with methoxy derivatives.¹³ Next, we performed blocking studies of [^{11}C]**32**. Co-injection of non-radioactive **32** (2 mg/kg) with [^{11}C]**32** resulted in significant inhibition of radioactivity in cerebellum ($P < 0.05$) as shown in Table 2. On the other hand, the uptake of radioactivity in cerebrum was not inhibited significantly. Furthermore cerebellum to blood ratio of [^{11}C]**32** was also significantly different between control and blocking studies. On the contrary, no significant difference was observed in cerebrum to blood ratio. It cannot be regarded that [^{11}C]**32** shows in vivo specific accumulation in cerebellum because of poor BBB permeability of [^{11}C]**32**. However certain specific binding site of [^{11}C]**32** may exist in the cerebellar glycine-binding site of the NMDA receptor. Finally, we examined the plasma protein-binding ratio of 4HQs, which was obtained by ultrafiltration method as shown in Figure 4. The plasma protein-binding ratio of [^{11}C]**32** was much lower than the methoxy analogs (71% vs 94–98%, respectively). Although these results indicate that the free fraction of [^{11}C]**32** is several fold higher than those of methoxy analogs, the brain uptake of [^{11}C]**32** was as low as those of methoxy analogs. It would appear that the reasons are in part because [^{11}C]**32** might be excreted from brain tissue by the efflux systems of BBB. The BBB permeability of various endogenous and exogenous ligands is regulated by efflux transporters such as P-glycoprotein (P-gp), organic anion transporter (OAT), and multidrug resistance protein.³⁰ It is reported that some radioligands for mapping neuroreceptors are substrates for P-gp.³¹ It has been shown that OAT3 is responsible for the elimination of several acidic drugs from the brain across the BBB.³² Although the pK_a value of **32** is calculated to be 5.59 which is much lower than those of methoxy analogs, **32** still has acidic moiety. It is unclear that which systems affect the permeability of [^{11}C]**32** across BBB. However it is possible that [^{11}C]**32** may be preferentially excreted from brain tissue by OAT. Another reason may be because

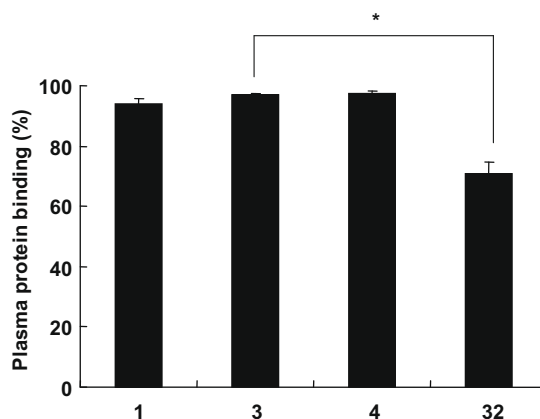


Figure 4. The plasma protein-binding ratio of 4HQs was obtained by ultrafiltration method after incubation of radioligand in rat plasma/buffer at 37 °C. Data are presented as the percentage (mean \pm SD, $n = 3$). * $P < 0.01$ (Kruskal–Wallis test, post test was Dunn's test).

[^{11}C]**32** still binds with plasma protein strongly and free fraction may be very low level.

Introduction of multiple basic groups and other electron-donating groups near the 4-position or non-acidic substituent in 4-position of 4HQs may increase significant higher pK_a values of 4-hydroxy group of 4HQs. As the results, plasma protein binding and efflux from organic anion transporter of 4HQs will be reduced, which is expected to improve BBB penetration. Further investigation is required for developing suitable in vivo imaging agents for the glycine site of the NMDA receptor.

3. Conclusion

We have developed high-affinity *N*-[^{11}C]Methylamino 4HQ derivatives **12** and **32** as new PET radioligand candidates for the glycine site of the NMDA receptor. In vitro autoradiography experiments imply that [^{11}C]**12** and [^{11}C]**32** showed high specific binding to the glycine site in the rat brain slices. In vivo studies using mice showed that both of these ligands have poor BBB permeability. Although the plasma protein-binding ratio of [^{11}C]**32** was much lower than the methoxy analogs, [^{11}C]**32** still binds with plasma protein strongly. Still acidic moiety and high affinity for plasma protein of [^{11}C]**32** may prevent the BBB penetration of [^{11}C]**32**. Further SAR studies are required for developing favorable PET ligands for the glycine site of the NMDA receptor with improved BBB permeability.

4. Experimental

4.1. General information

Proton nuclear magnetic resonance (^1H NMR) spectra were recorded on a JEOL GX-270 spectrometer and a Varian UNITY INOVA 400. Mass spectra (MS) were obtained on a JOEL TMS-D300 spectrometer or an Applied Biosystem Mariner System 5299 spectrometer by use of electrospray ionization (ESI) or fast atom bombardment (FAB). High-resolution mass spectra (HRMS) were obtained on a QSTAR[®]XL MS/MS System by use of ESI. Infrared (IR) spectra were recorded with a JASCO IR Report-100 spectrometer. Column chromatography was done on Merck Kieselgel 60 (70–230 mesh), and analytical thin layer chromatography (TLC) was carried out on Silica Gel 60 F₂₅₄ plates (Merck). In the synthetic procedures, organic extracts were routinely dried over anhydrous Na_2SO_4 and evaporated with a rotatory evaporator

under reduced pressure. High-performance liquid chromatography (HPLC) was done using a Waters HPLC system for non-radioactive runs or a JASCO HPLC system for radioactive runs. Effluent radioactivity from the HPLC was determined using a NaI (TI) scintillation detector system. Carbon-11 was generated by the $^{14}\text{N}(\text{p}, \alpha)^{11}\text{C}$ nuclear reaction using a CYPRIS HM-18 cyclotron (Sumitomo Heavy Industries, Ltd). Preparation of $[^{11}\text{C}]\text{CH}_3\text{I}$, $[^{11}\text{C}]\text{CH}_3\text{OTf}$ and subsequent ^{11}C -methylation were carried out automatically by using a synthetic apparatus for ^{11}C -labeled compounds in National Institute of Radiological Sciences (NIRS). Radioactivity was quantified with an IGC-3R Curiometer (Aloka). $[^{11}\text{C}]\mathbf{1}$, $[^{11}\text{C}]\mathbf{3}$, and $[^{11}\text{C}]\mathbf{4}$ were prepared as described in the literature.^{7,13} All reagents were used as received unless otherwise stated. The animal experiments were carried out according to the recommendations of the committee for the care and use of laboratory animals, NIRS.

4.1.1. Methyl 4-chloro-2-(3-(4-nitrobenzyl)phenylacetamide) benzoate (**7**)

Methyl 4-chloro-2-(3-(bromomethyl) phenylacetamido) benzoate (**6**)¹⁴ (2.4 g, 6.03 mmol), 4-nitrophenylboronic acid (1.51 g, 9.05 mmol), and tetrakis(triphenyl)phosphine palladium(0) (70 mg, 0.06 mmol) were stirred in dimethoxyethane (10 ml) for 10 min, then 2 M aqueous sodium carbonate (9.7 ml, 18.09 mmol) was added, and stirred at 90 °C. After 4 h, EtOAc (30 ml) was added to the mixture, the organic layer was separated, and the aqueous layer extracted with EtOAc (20 ml). The combined organic layers were washed with water and brine, dried with Na_2SO_4 , and evaporated to dryness. The crude product was chromatographed on silica gel with hexane/EtOAc = 4:1 to provide **7** (2.5 g, 95%) as a white solid. mp = 106–107 °C, ^1H NMR (CDCl_3) δ : 11.10 (1H, s), 8.81 (1H, d, J = 2.0 Hz), 8.36 (2H, d, J = 8.7 Hz), 8.12 (1H, d, J = 8.6 Hz), 7.92 (1H, d, J = 8.6 Hz), 7.78 (2H, d, J = 8.8 Hz), 7.35 (1H, d, J = 8.6 Hz), 7.32 (1H, t, J = 7.5 Hz), 7.20 (1H, s), 7.04 (1H, dd, J = 8.6, 2.1 Hz), 4.09 (2H, s), 3.86 (3H, s), 3.73 (2H, s), IR (CHCl_3) cm^{-1} : 2910, 1687, 1590, ESI-MS m/z ; 349 (M+H)⁺.

4.1.2. Methyl 4-chloro-2-(3-(4-aminobenzyl)phenylacetamide) benzoate (**8**)

To a solution of **7** (2.4 g, 5.47 mmol) in THF (100 ml) was added dropwise a solution of 20% TiCl_3 in hydrochloric acid (40 ml, 62.17 mmol) and stirred at room temperature. After 24 h, the mixture was cooled in an ice bath and neutralized with aqueous 10% NaOH. The resulting dark slurry was diluted with EtOAc (500 ml) and the mixture was stirred vigorously until the precipitation became yellow. The suspension was filtered, and the residue was washed with EtOAc. The filtrate was washed with water and brine, dried with Na_2SO_4 , and evaporated to dryness. The crude product was chromatographed on silica gel with hexane/EtOAc = 2:1 to provide **8** (1.97 g, 85%) as a colorless oil, ^1H NMR (CDCl_3) δ : 11.04 (1H, br s), 8.82 (1H, d, J = 2.0 Hz), 7.91 (1H, d, J = 8.6 Hz), 7.26 (1H, t, J = 7.3 Hz), 7.19 (1H, d, J = 7.1 Hz), 7.18 (2H, d, J = 7.3 Hz), 7.10 (1H, d, J = 7.3 Hz), 7.03 (1H, dd, J = 8.6, 2.1 Hz), 6.98 (2H, d, J = 8.2 Hz), 6.60 (2H, d, J = 8.2 Hz), 3.89 (2H, s), 3.84 (3H, s), 3.71 (2H, s), 3.56 (2H, br s), IR (CHCl_3) cm^{-1} : 3246, 3001, 1687, 1578, FAB-MS m/z ; 409 (M+H)⁺.

4.1.3. 7-Chloro-4-hydroxy-3-{3-(4-aminobenzyl)phenyl}-2-(1H)-quinolone (**9**)

To a solution of **8** (135 mg, 0.33 mmol) in DMSO (3 ml) was added anhydrous potassium carbonate (227 mg, 1.64 mmol) and stirred at 80 °C. After 6 h, MeOH (2 ml) was added to the mixture, followed by 1 M HCl to maintain at pH 7–8 in order to give a white precipitate. The solid was collected, washed with ethanol and ether, and dried to give **9** (96 mg, 77%) as a white solid, mp = 228–230 °C, ^1H NMR (DMSO) δ : 11.49 (1H, s), 7.91 (1H, d,

J = 8.6 Hz), 7.30 (1H, d, J = 1.5 Hz), 7.25 (1H, t, J = 7.4 Hz), 7.19 (1H, dd, J = 8.6, 1.9 Hz), 7.16 (1H, s), 7.13 (1H, d, J = 7.6 Hz), 7.10 (1H, d, J = 7.5 Hz), 6.90 (2H, d, J = 8.5 Hz), 6.48 (2H, d, J = 8.2 Hz), 3.77 (3H, s), IR (KBr) cm^{-1} : 3400–3000, 2922, 1650, 1582, FAB-MS (m/z); 377 (M+H)⁺.

4.1.4. Methyl 4-chloro-2-(3-(4-methylaminobenzyl)phenylacetamide) benzoate (**10**) and methyl 4-chloro-2-(3-(4-dimethylaminobenzyl)phenylacetamide) benzoate (**11**)

To a solution of **8** (947 mg, 2.32 mmol) in DMF/EtOH (1:1, 10 ml), CH_3I (0.14 ml, 2.32 mmol) was added and stirred at room temperature. After 5 h, EtOAc (50 ml) was added to the mixture, washed with brine, dried with Na_2SO_4 , and evaporated to dryness. The crude product was chromatographed on silica gel with hexane/EtOAc = 3:1 to provide **10** (176 mg, 23%) as a colorless oil and **11** (220 mg, 32%) as a colorless oil.

Compound 10: ^1H NMR (CDCl_3) δ : 11.03 (1H, br s), 8.82 (1H, d, J = 2.1 Hz), 7.90 (1H, d, J = 8.7 Hz), 7.27 (1H, t, J = 7.5 Hz), 7.19 (1H, s), 7.17 (1H, d, J = 7.6 Hz), 7.10 (1H, d, J = 7.5 Hz), 7.02 (1H, dd, J = 8.6, 2.1 Hz), 7.01 (2H, d, J = 8.5 Hz), 6.53 (2H, d, J = 8.5 Hz), 3.89 (2H, s), 3.84 (3H, s), 3.71 (2H, s), 2.81 (3H, s), IR (KBr) cm^{-1} : 3200, 2916, 1689, 1578, FAB-MS (m/z); 423.2 (M+H)⁺.

Compound 11: ^1H NMR (CDCl_3) δ : 11.04 (1H, br s), 8.82 (1H, d, J = 2.0 Hz), 7.91 (1H, d, J = 8.6 Hz), 7.27 (1H, d, J = 7.5 Hz), 7.21 (1H, s), 7.19 (1H, d, J = 7.4 Hz), 7.11 (1H, d, J = 7.3 Hz), 7.06 (2H, d, J = 8.7 Hz), 7.03 (1H, dd, J = 8.6, 2.1 Hz), 6.66 (2H, d, J = 8.6 Hz), 3.90 (2H, s), 3.83 (3H, s), 3.71 (2H, s), 2.90 (6H, s), IR (KBr) cm^{-1} : 3300, 2900, 1690, 1578, FAB-MS (m/z); 437 (M+H)⁺.

4.1.5. 7-Chloro-4-hydroxy-3-{3-(4-methylaminobenzyl)phenyl}-2-(1H)-quinolone (**12**)

Following the above procedure for **9** starting from compound **10**, the title compound **12** (96 mg, 97%) was obtained as a white solid, mp = 261–263 °C, ^1H NMR (DMSO) δ : 11.44 (1H, s), 10.19 (1H, br s), 7.90 (1H, d, 8.6 Hz), 7.29 (1H, d, J = 1.9 Hz), 7.26 (1H, t, J = 7.7 Hz), 7.20–7.17 (3H, m), 7.14 (1H, d, J = 7.3 Hz), 7.09 (1H, d, J = 7.6 Hz), 6.97 (2H, d, J = 8.4 Hz), 6.45 (2H, d, J = 8.4 Hz), 5.38 (1H, br s), 3.79 (2H, s), 2.61 (3H, s), IR (KBr) cm^{-1} : 3421, 3200–2800, 1647, 1581, ESI-HRMS (m/z) calcd for $\text{C}_{23}\text{H}_{20}\text{ClN}_2\text{O}_2$, 391.121 (M+H)⁺, obsd 391.1221.

4.1.6. 7-Chloro-4-hydroxy-3-{3-(4-dimethylaminobenzyl)phenyl}-2-(1H)-quinolone (**13**)

Following the above procedure for **9** starting from compound **11**, the title compound **13** (143 mg, 95%) was obtained as a white solid, mp = 253–255 °C, ^1H NMR (DMSO) δ : 11.48 (1H, s), 10.21 (1H, br s), 7.91 (1H, d, 8.6 Hz), 7.30 (1H, d, J = 1.9 Hz), 7.28 (1H, t, J = 7.5 Hz), 7.19 (1H, dd, J = 8.8, 2.0 Hz), 7.17 (1H, s), 7.14 (1H, d, J = 8.1 Hz), 7.11 (1H, d, J = 7.9 Hz), 7.06 (2H, d, J = 8.4 Hz), 6.64 (2H, d, J = 8.6 Hz), 3.83 (2H, s), 2.82 (6H, s), IR (KBr) cm^{-1} : 3410, 3300–2800, 1647, 1581, ESI-HRMS (m/z) calcd for $\text{C}_{24}\text{H}_{22}\text{ClN}_2\text{O}_2$, 405.1370 (M+H)⁺, obsd 405.1369.

4.1.7. Methyl 2-(3-nitrophenyl) acetamide-4-chlorobenzoate (**16**)

To a solution of 3-nitrophenyl acetic acid (1.63 g, 9.81 mmol) in CH_2Cl_2 (10 ml), 2 M dichloromethane solution of oxalyl chloride (6.5 ml, 13.0 mmol) was added and stirred at room temperature. After 6 h, the mixture was evaporated and the residue was dissolved in dichloroethane (10 ml); and methyl-2-amino-4-chlorobenzoate (**14**) (800 mg, 4.31 mmol) was added. The mixture was refluxed for 5 h, cooled to room temperature, quenched by the addition of saturated aqueous sodium hydrogen carbonate, and extracted with CHCl_3 . The organic layer was washed with brine, dried with Na_2SO_4 , and evaporated to dryness. The crude product was chromatographed on silica gel with hexane/ CHCl_3 = 1:3 to provide

16 as (1.29 g, 86%) a white solid, mp = 125–126 °C, $^1\text{H NMR}$ (CDCl_3) δ : 11.30 (1H, s), 8.78 (1H, d, 2.1 Hz), 8.27 (1H, t, J = 1.8 Hz), 8.19 (1H, d, J = 7.9 Hz), 7.94 (1H, d, J = 8.6 Hz), 7.72 (1H, d, J = 7.5 Hz), 7.56 (1H, t, 8.0 Hz), 7.07 (1H, dd, 8.6, 2.6 Hz), 3.89 (3H, s), 3.87 (2H, s). IR (KBr) cm^{-1} : 3249, 1701, 1689, 1521, FAB-MS (m/z): 349 ($\text{M}+\text{H}$) $^+$.

4.1.8. Methyl 2-(3-aminophenyl) acetamide-4-chlorobenzoate (17)

To a solution of **16** (3.5 g, 10.04 mmol) in AcOH/EtOH (2:7, 45 ml), iron powder (3.36 g, 60.16 mmol) was added and stirred at 80 °C. After 6 h, the mixture was cooled to room temperature, added to water (200 ml), and filtered. The filtrate was extracted with EtOAc, washed with brine dried with Na_2SO_4 , and evaporated to dryness. The crude product was chromatographed on silica gel with $\text{CHCl}_3/\text{EtOAc}$ = 10:1 to provide **17** (3.1 g, 97%) as a yellow oil, $^1\text{H NMR}$ (DMSO) δ : 10.69 (1H, s), 8.46 (1H, d, 2.0 Hz), 7.91 (1H, d, J = 8.7 Hz), 7.24 (1H, dd, J = 8.6, 2.0 Hz), 6.98 (1H, d, J = 8.6 Hz), 6.53–6.46 (3H, m), 5.14 (2H, br s), 3.79 (3H, s), 3.56 (2H, s). IR (KBr) cm^{-1} : 3362, 3263, 1684, 1652, ESI-MS (m/z): 319 ($\text{M}+\text{H}$) $^+$.

4.1.9. Methyl 4-chloro-2-3-(4-methoxyphenylamino)-phenylacetamido-benzoate (18)

To a solution of 4-methoxyphenylboronic acid (2.14 g, 14.08 mmol) in toluene (10 ml), a solution of **17** (3.0 g, 9.41 mmol) in toluene (5 ml), copper(II) acetate (171 mg, 0.94 mmol), myristic acid (430 mg, 1.88 mmol), and 2,6-lutidine (1.1 ml, 9.42 mmol) was mixed. The mixture was stirred for 24 h at room temperature, then EtOAc (50 ml) was added, washed with brine dried with Na_2SO_4 , and evaporated to dryness. The crude product was chromatographed on silica gel with hexane/EtOAc = 3:1 to provide **18** (2.96 g, 74%) as a brown solid, mp = 89–90 °C, $^1\text{H NMR}$ (CDCl_3) δ : 11.05 (1H, br s), 8.82 (1H, d, J = 2.1 Hz), 7.91 (1H, d, 8.6 Hz), 7.24–7.06 (3H, m), 7.03 (1H, dd, J = 8.6, 2.1 Hz), 7.00–6.84 (5H, m), 3.86 (3H, s), 3.76 (3H, s), 3.67 (2H, s), IR (KBr) cm^{-1} : 3412, 2916, 1705, 1598, ESI-MS (m/z): 425 ($\text{M}+\text{H}$) $^+$.

4.1.10. 7-Chloro-4-hydroxy-3-(3-(4-methoxyphenylamino)-phenyl)-2(1H)-quinolone (19)

To a solution of **18** (890 mg, 2.09 mmol) in THF (15 ml), potassium hexamethyldisilazide (9.1 ml of 15% solution in toluene, 6.27 mmol) was added and stirred at room temperature. After 5 h, the reaction mixture was quenched by the addition of MeOH (5 ml) followed by TFA to maintain at pH 7–8, then EtOAc (20 ml) was added, washed with brine, dried with Na_2SO_4 , and evaporated to dryness. The crude product was chromatographed on silica gel with $\text{CHCl}_3/\text{MeOH}$ = 15:1 to provide **19** (780 mg, 98%) as a white solid, mp = 269–271 °C, $^1\text{H NMR}$ (DMSO) δ : 11.48 (1H, s), 10.13 (1H, br s), 7.89 (1H, d, J = 8.6 Hz), 7.83 (1H, d, J = 2.1 Hz), 7.29 (1H, d, J = 2.0 Hz), 7.19 (1H, d, J = 8.6 Hz), 7.18 (1H, t, J = 7.0 Hz), 7.08–7.01 (2H, m), 6.92–6.83 (3H, m), 6.70 (1H, d, J = 7.5 Hz), 3.69 (3H, s), IR (KBr) cm^{-1} : 3383, 2918, 1598, ESI-HRMS (m/z) calcd for $\text{C}_{22}\text{H}_{18}\text{ClN}_2\text{O}_3$; 393.1006 ($\text{M}+\text{H}$) $^+$, obsd 393.1012.

4.1.11. Methyl 2-(3-methoxyphenyl)acetamide-4-chloro-6-nitrobenzoate (22)

Following the above procedure for **16** starting from compound **20**¹⁶ and **21**, the title compound **22** (1.76 g, 95%) was obtained as a white solid, mp = 96–98 °C, $^1\text{H NMR}$ (CDCl_3) δ : 9.19 (1H, br s), 8.78 (1H, d, J = 2.1 Hz), 7.51 (1H, d, 2.0 Hz), 7.34 (1H, t, J = 1.9 Hz), 6.93–6.85 (3H, m), 3.84 (3H, s), 3.74 (5H, s), IR (KBr)

cm^{-1} : 3250, 1736, 1670, 1652, ESI-MS (m/z): 379 $\{(\text{M}+\text{H})^+$ for $^{35}\text{Cl}\}$, 381 $\{(\text{M}+\text{H})^+$ for $^{37}\text{Cl}\}$.

4.1.12. Methyl 2-(3-methoxyphenyl)acetamide-6-amino-4-chlorobenzoate (23)

Following the above procedure for **17** starting from compound **22**, the title compound **23** (1.76 g, 95%) was obtained as a white solid, mp = 90–93 °C, $^1\text{H NMR}$ (CDCl_3) δ : 10.52 (1H, br s), 8.01 (1H, d, J = 1.9 Hz), 7.29 (1H, t, 7.8 Hz), 6.93 (1H, d, J = 7.5 Hz), 6.89 (1H, s), 6.86 (1H, d, J = 8.1 Hz), 6.37 (1H, d, J = 2.0 Hz), 5.44 (2H, s), 3.82 (3H, s), 3.73 (3H, s), 3.71 (2H, s), IR (KBr) cm^{-1} : 3500, 3363, 1734, 1670, 1609, ESI-MS (m/z): 349 $\{(\text{M}+\text{H})^+$ for $^{35}\text{Cl}\}$, 351 $\{(\text{M}+\text{H})^+$ for $^{37}\text{Cl}\}$.

4.1.13. 5-Amino-7-chloro-4-hydroxy-3-(3-methoxyphenyl)-2(1H)-quinolone (24)

Following the above procedure for **9** starting from compound **23**, the title compound **24** (89 mg, 98%) was obtained as a white solid, mp = 263–265 °C, $^1\text{H NMR}$ (DMSO) δ : 11.15 (1H, br s), 7.79 (2H, br s), 7.29 (1H, d, J = 7.7 Hz), 6.87–6.84 (3H, m), 6.40 (1H, d, J = 1.8 Hz), 6.32 (1H, d, J = 1.7 Hz), 3.32 (3H, s), IR (KBr) cm^{-1} : 3503, 3396, 3200–2700, 1647, 1605, ESI-HRMS (m/z) calcd for $\text{C}_{16}\text{H}_{14}\text{ClN}_2\text{O}_3$; 317.0693 ($\text{M}+\text{H}$) $^+$, obsd 317.0700 ($\text{M}+\text{H}$) $^+$.

4.1.14. 5-Methylamino-7-chloro-4-hydroxy-3-(3-methoxyphenyl)-2(1H)-quinolone (25)

To a solution of **24** (52 mg, 0.16 mmol) in MeOH (1 ml), 37% formaldehyde/ H_2O (9.8 μl , 0.131 mmol) was added, followed by sodium cyanoborohydride (8.5 mg, 0.131 mmol) and stirred at room temperature. After 10 h, the reaction mixture was quenched with water (1 ml), extracted with EtOAc, washed with brine, dried with Na_2SO_4 , and evaporated to dryness. The crude product was chromatographed on silica gel with $\text{CHCl}_3/\text{MeOH}$ = 15:1 to provide **25** (38 mg, 71%) as a yellow solid, mp = 261–263 °C, $^1\text{H NMR}$ (DMSO) δ : 11.00 (1H, s), 7.24 (1H, t, 7.7 Hz), 6.93–6.79 (3H, m), 6.44 (1H, d, J = 1.9 Hz), 6.08 (1H, d, J = 1.8 Hz), 3.73 (3H, s), 2.77 (3H, s), ESI-HRMS (m/z) calcd for $\text{C}_{17}\text{H}_{16}\text{ClN}_2\text{O}_3$, 331.0849 ($\text{M}+\text{H}$) $^+$, obsd 331.0869 ($\text{M}+\text{H}$) $^+$.

4.1.15. Methyl 2-(3-methoxyphenyl)acetamide-4-chloro-6-dimethylamino benzoate (26)

To an ice cooled solution of 37% formaldehyde/ H_2O (0.145 ml, 1.9 mmol) 3 M of aqueous H_2SO_4 (0.26 ml) was added a slurry of **25** (110 mg, 0.32 mmol) and sodium borohydride (84 mg, 2.22 mmol) in THF (1 ml). The mixture was stirred at room temperature for 2 h, then quenched with 10% aqueous NaOH (5 ml), extracted with EtOAc, washed with brine, dried with Na_2SO_4 , and evaporated to dryness. The crude product was chromatographed on silica gel with $\text{CHCl}_3/\text{MeOH}$ = 40:1 to provide **26** (102 mg, 86%) as a colorless oil, $^1\text{H NMR}$ (CDCl_3) δ : 9.16 (1H, br s), 7.95 (1H, d, 1.9 Hz), 7.30 (1H, t, J = 7.5 Hz), 6.91 (1H, d, J = 7.1 Hz), 6.87 (1H, d, J = 6.7 Hz), 6.60 (1H, d, J = 1.9 Hz), 3.83 (3H, s), 3.74 (3H, s), 3.68 (2H, s), 2.78 (6H, s), IR (KBr) cm^{-1} : 3363, 2939, 1684, 1595, ESI-MS (m/z): 377 $\{(\text{M}+\text{H})^+$ for $^{35}\text{Cl}\}$, 379 $\{(\text{M}+\text{H})^+$ for $^{37}\text{Cl}\}$.

4.1.16. 5-Dimethylamino-7-chloro-4-hydroxy-3-(3-methoxyphenyl)-2(1H)-quinolone (27)

Following the above procedure for **9** starting from compound **26**, the title compound **27** (89 mg, 98%) was obtained as a white solid, mp = 208–210 °C, $^1\text{H NMR}$ (DMSO) δ : 11.42 (1H, br s), 7.49 (1H, t, 1.9 Hz), 7.24 (1H, t, J = 8.0 Hz), 7.21 (1H, d, J = 1.8 Hz), 7.02 (1H, d, J = 7.9 Hz), 7.00 (1H, d, J = 2.4 Hz), 6.81 (1H, dd, J = 8.2, 2.1 Hz), 3.74 (3H, s), 2.76 (6H, s), IR (KBr) cm^{-1} : 3380, 2927, 1635, ESI-HRMS (m/z) calcd for $\text{C}_{18}\text{H}_{18}\text{ClN}_2\text{O}_3$, 345.1006 ($\text{M}+\text{H}$) $^+$, obsd 345.1003 ($\text{M}+\text{H}$) $^+$.

4.1.17. Methyl 2-(3-nitrophenyl)acetamide-4-chloro-6-ethylbenzoate (29)

Following the above procedure for **16** starting from compound **28**¹⁷ and **15**, the title compound **29** (334 mg, 65%) was obtained as a white solid, mp = 85–86 °C, ¹H NMR (DMSO) δ: 9.72 (1H, s), 8.34 (1H, d, *J* = 2.2 Hz), 8.22–8.19 (2H, m), 7.71 (1H, d, *J* = 8.0 Hz), 7.57 (1H, d, *J* = 7.9 Hz), 6.99 (1H, d, *J* = 2.1 Hz), 3.85 (3H, s), 3.82 (2H, s), 2.74 (2H, q, *J* = 7.5 Hz), 1.17 (3H, t, *J* = 7.5 Hz), IR (KBr) cm⁻¹: 3244, 1722, 1670, 1529, ESI-MS (*m/z*); 377 (M+H)⁺.

4.1.18. 5-Ethyl-7-chloro-4-hydroxy-3-(3-nitrophenyl)-2(1H)-quinolone (30)

Following the above procedure for **19** starting from compound **29**, the title compound **30** (193 mg, 87%) was obtained as a white solid, mp = 232–233 °C, ¹H NMR (DMSO) δ: 11.62 (1H, s), 10.42 (1H, br s), 8.20–8.17 (2H, m), 7.80 (1H, d, *J* = 7.6 Hz), 7.69 (1H, t, *J* = 7.9 Hz), 7.23 (1H, d, *J* = 2.2 Hz), 7.03 (1H, d, *J* = 2.2 Hz), 3.14 (2H, q, *J* = 7.4 Hz), 1.20 (3H, t, *J* = 7.4 Hz), IR (KBr) cm⁻¹: 3377, 1681, 1635, FAB-MS (*m/z*); 345 (M+H)⁺.

4.1.19. 3-(3-Aminophenyl)-7-chloro-4-hydroxy-2(1H)-quinolone (31)

Following the above procedure for **17** starting from compound **30**, the title compound **31** (489 mg, 91%) was obtained as a white solid, mp = 178–179 °C, ¹H NMR (DMSO) δ: 11.44 (1H, br s), 9.92 (1H, s), 7.62 (1H, d, *J* = 8.1 Hz), 7.30 (1H, t, *J* = 7.8 Hz), 7.19 (1H, t, *J* = 2.2 Hz), 7.05–6.96 (2H, m), 3.12 (2H, q, *J* = 7.3 Hz), 1.18 (3H, t, *J* = 7.2 Hz), IR (KBr) cm⁻¹: 3480, 3300, 1683, 1635, FAB-MS (*m/z*); 315 (M+H)⁺.

4.1.20. 5-Ethyl-7-chloro-4-hydroxy-3-(3-methylaminophenyl)-2(1H)-quinolone (32) and 5-ethyl-7-chloro-4-hydroxy-3-(3-dimethylaminophenyl)-2(1H)-quinolone (33)

Following the above procedure for **10** and **11** starting from compound **31**, the title compounds **32** (3.5 mg, 17%) and **33** (1.8 mg, 8%) were obtained as white solid, respectively.

Compound 32: mp = 196–198 °C, ¹H NMR (DMSO) δ: 11.31 (1H, s), 9.47 (1H, s), 7.17 (1H, s), 7.11 (1H, t, *J* = 2.5 Hz), 6.95 (1H, s), 6.49–6.47 (3H, m), 5.55 (1H, s), 3.11 (2H, q, *J* = 7.0 Hz), 2.67 (3H, s), 1.17 (3H, t, *J* = 7.4 Hz), IR (KBr) cm⁻¹: 3280, 3000, 1670, 1590, ESI-HRMS (*m/z*) calcd for C₁₈H₁₈ClN₂O₂, 329.1057 (M+H)⁺, obsd 329.1069.

Compound 33: mp = 203–205 °C, ¹H NMR (DMSO) δ: 11.40 (1H, s), 9.48 (1H, s), 8.36 (1H, s), 7.19 (1H, s), 6.98 (1H, d, *J* = 2.3 Hz), 6.71 (1H, d, *J* = 7.6 Hz), 6.64 (1H, s), 6.59 (1H, d, *J* = 7.1 Hz), 3.11 (2H, q, *J* = 7.2 Hz), 2.89 (6H, s), 1.18 (3H, t, *J* = 7.2 Hz), IR (KBr) cm⁻¹: 3350, 3010, 1692, 1610, ESI-HRMS (*m/z*) calcd for C₁₉H₂₀ClN₂O₂, 343.1213 (M+H)⁺, obsd 343.1219.

4.2. Radiosynthesis

4.2.1. 7-Chloro-4-hydroxy-3-(3-(4-[¹¹C]methylaminobenzyl)phenyl)-2(1H)-quinolone ([¹¹C]**12**)

[¹¹C]CH₃OTf was prepared using general method as described in the literature.³³ [¹¹C]CH₃OTf was trapped in an anhydrous acetone (250 μl) containing **9** (0.5 mg, 1.34 μmol) at –15 to –20 °C. The reaction vessel was heated at 60 °C and kept there for 1.5 min. After addition of an HPLC mobile phase (600 μl) and DMF (400 μl), the radioactive mixture was transferred onto an HPLC (Cosmosil 5C₁₈-AR II, 10 × 250 mm, Nacalai) and eluted with CH₃CN/H₂O = 50:50 at a flow rate of 4.0 ml/min. A radioactive fraction having a retention time of 11 min was collected in a flask containing Tween 80 (75 μl) and ethanol (150 μl). After evaporation of the solvents under reduced pressure, the radioactive residue was dissolved in sterile distilled water (5 ml) to give [¹¹C]**12** as an aqueous solution. Radiochemical purity was assayed to be >98% by ana-

lytical HPLC (column; Nacalai Cosmosil 5C₁₈-ARII, 4.6 × 250 mm, mobile phase; CH₃CN/H₂O = 50:50, flow rate; 1.0 ml/min). The specific activity of purified [¹¹C]**12** was calculated by UV spectroscopy (254 nm) to be 47 GBq/μmol. The total synthesis and purification time was 27 min with an overall decay corrected yield of 8%.

4.2.2. 5-Ethyl-7-chloro-4-hydroxy-3-(3-[¹¹C]methylaminophenyl)-2(1H)-quinolone ([¹¹C]**32**)

[¹¹C]Methylation of **31** (0.7 mg, 2.2 μmol) was carried out by the same manner as described above. The radioactive fraction having a retention time of 13 min from HPLC (column; Nacalai COSMOSIL 5C₁₈-ARII, 10 × 250 mm, mobile phase; CH₃CN/H₂O = 50:50, flow rate; 4.0 ml/min) was collected, evaporated, and dissolved in sterile distilled water to give radiochemically pure (>98%) [¹¹C]**32**. The specific activity of purified was 63 GBq/μmol. The total synthesis and purification time was 29 min with an overall decay corrected yield of 27%.

4.3. In vitro binding assays

The purity of test compounds were assayed to be >97% by analytical HPLC (column; Nacalai Cosmosil 5C₁₈-AR 300, 4.6 × 250 mm, mobile phase; MeOH/H₂O = 80:20–45:55, flow rate; 1.0 ml/min). The *K_i* values of 4HQs for binding of [³H]MDL-105,519 to rat cortical membrane homogenates in 50 mM Tris-HCl buffer were determined by the method in the literature.¹⁸ In brief, well-washed membranes (125 μg protein) in 50 mM Tris-HCl buffer, pH 8.0, were incubated with [³H]MDL-105,519 (2 nM) with either buffer or displacing drug to a final volume of 500 μl for 45 min at 4 °C. Non-specific binding was defined by the addition of unlabeled glycine at 100 μM. Bound ligand was collected by rapid filtration using a Brandel cell harvester onto glass fiber filter (GF/B). The filters were washed rapidly three times with 2.5 ml of ice-cold assay buffer. Following separation and rinsed, the filters were placed into scintillation liquid (4 ml; ASCII, GE Healthcare Bio-Sciences) and radioactivity was determined with a liquid scintillation counter.

4.4. In vitro receptor autoradiography

The brain sagittal sections obtained by the method in the literature²¹ were pre-incubated for 30 min at 25 °C in 50 mM Tris-HCl buffer (pH 7.4 at 25 °C), and subsequently incubated in the same buffer containing [¹¹C]**12** or [¹¹C]**32** (1.59–2.13 nM) at 25 °C for 30 min. The slices were rinsed twice for 3 min each with cold (5 °C) incubation buffer, and subsequently dipped into cold water. The sections were dried under a steam of warm air and placed in contact with ¹¹C-sensitive imaging plates (BAS-SR 127, Fuji Photo Film) for 60 min. Distributions of radioactivity on the plates were analyzed by FUJIX BAS 5000 bioimaging analyzer (Fuji Photo Film Co, Ltd), which was photographically visualized as shown in Figure 2A–D. Regions of interest (ROIs) on the slices were placed on the cerebral cortex, hippocampus, striatum, thalamus, and cerebellum; and the radioactivities in these regions were expressed as photo-stimulated luminescence (PSL) values on ROI-background PSL value per square millimeter. The specific binding was determined as the difference between total binding and binding in the presence of the corresponding non-radioactive 4-hydroxyquinolones (10 μM).

4.5. Drug inhibition for in vitro binding

The brain slices were incubated at 25 °C for 30 min in 50 mM Tris-HCl buffer (pH 7.4 at 25 °C) containing [¹¹C]4HQ (1.59–2.13 nM) with or without drugs (10 μM for antagonist and 1 mM for agonist). Following the incubation, the sections were rinsed, dried, and apposed to the imaging plates for 60 min by

the same manner as described above. The PSL data corresponding to the hippocampus in the presence of drugs were divided by the respective control PSL data in the absence of drugs. The obtained % total binding values were averaged in at least triplicate sections from three animals and shown in Figure 3A (agonist) and B (antagonist).

4.6. In vivo brain distribution and metabolism

The [^{11}C]12 or [^{11}C]32 (0.2 ml, ca. 7.4 MBq) was injected intravenously via tail vein into ddY mice (35–45 g). These mice were killed at 1 min or 30 min by decapitation. The whole brains were rapidly removed; and the cerebrum and cerebellum were dissected. The obtained tissue and blood samples were weighed and their radioactivities were measured with a Packard γ -counter and corrected for decay. The results were expressed as the percent of injected dose per gram of tissue (% dose/g) (Table 2). To assess the in vivo specific binding of [^{11}C]32, non-radioactive 32 (2 mg/kg) was mixed with [^{11}C]32 and injected into mice. To assess the metabolism of [^{11}C]32 in mouse blood and brain, the mice were killed at 30 min after [^{11}C]32 (40 MBq) injection. Whole brains were quickly removed, homogenized with ice-cooled MeOH (2 ml), and centrifuged at 10,000 rpm for 1 min at 4 °C. The metabolites in MeOH extract were analyzed by radio-TLC using a $\text{CHCl}_3/\text{CH}_3\text{CN} = 3:1$ ($R_f = 0.3$), $\text{CHCl}_3/\text{MeOH} = 9:1$ ($R_f = 0.5$), CH_3CN ($R_f = 0.7$), as mobile phases.

4.7. Partition coefficient determination

Partition coefficient between *n*-octanol and buffer was measured by a conventional shake flask method in triplicate as follows. The 4HQs (1–2 mg) were well shaken in a mixture of *n*-octanol (1 ml) and 10 mM phosphate buffer (pH 7.4, 1 ml) for 15 min at ambient temperature. After centrifugation (2500 rpm for 5 min) of the mixture, the two layers were separated and analyzed by HPLC (column; Nacalai Cosmosil 5C₁₈-AR 300, 4.6 × 250 mm, mobile phase; MeOH/H₂O = 70:30–65:35, flow rate; 1.0 ml/min) to obtain log *D* (pH 7.4) values (Table 1).

4.8. Plasma protein-binding assay

The plasma protein-binding ratios of [^{11}C]4HQ were evaluated by ultrafiltration according to the method in the literature.^{34,35} In brief, 10-fold dilution of the rat serum with 66 mM phosphate buffer (pH 7.4) containing [^{11}C]4HQ (0.67–0.89 MBq, 500 μl) was incubated for 30 min at 30 °C. Subsequently, the plasma was transferred to a Centrifree® Centrifugal Filter Device (Amicon Bioseparations, Millipore) and centrifuged at 2000 rpm for 15 min. Radioactivity in whole plasma and in the filtrate was measured using a Packard γ -counter. The fraction bound to protein was calculated by subtracting the unbound filtrate from 100%.

4.9. Data analysis

Data are expressed as the mean \pm standard deviation. Regional brain uptake of [^{11}C] ligands were statistically analyzed using non-parametric analysis (Mann–Whitney *U*-test) as shown in Table 2. The plasma protein-binding ratios of 4HQs were analyzed by the Kruskal–Wallis test with Dunn's multiple comparison post-test as shown in Figure 4. A value of *P* < 0.05 was considered statistically significant.

Acknowledgments

The authors gratefully acknowledge the assistance of Mr. Nengaki and Mr. Ogawa, Sumitomo Accelerator Services, and Mr. Takei, Tokyo Nuclear Service, in conducting the radiosyntheses. We are also grateful to the cyclotron crew of the NIRS for their technical support. The studies were supported by Grant-in-Aid for Young Scientists (Start-up) (18890080).

References and notes

- Danysz, W.; Parsons, C. G. *Pharmacol. Rev.* **1998**, *50*, 597.
- Parsons, C. G.; Danysz, W.; Quack, G. *Drug News Perspect.* **1998**, *11*, 523.
- Millan, M. J. *Psychopharmacology* **2005**, *179*, 30.
- Shim, S. S.; Hammonds, M. D.; Kee, B. S. *Eur. Arch. Psychiatry Clin. Neurosci.* **2008**, *258*, 16.
- Haradahira, T.; Zhang, M.-R.; Maeda, J.; Okauchi, T.; Kida, T.; Kawabe, K.; Sasaki, S.; Suhara, T.; Suzuki, K. *Chem. Pharm. Bull.* **2001**, *49*, 147.
- Matsumoto, R.; Haradahira, T.; Ito, H.; Fujimura, Y.; Seki, C.; Ikoma, Y.; Maeda, J.; Arakawa, R.; Takano, A.; Takahashi, H.; Higuchi, M.; Suzuki, K.; Fukui, K.; Suhara, T. *Synapse* **2007**, *61*, 795.
- Haradahira, T.; Suzuki, K. *Nucl. Med. Biol.* **1999**, *26*, 245.
- Opacka-Juffry, J.; Morris, H.; Ashworth, S.; Osman, S.; Hirani, E.; Macleod, A. M.; Luthra, S. K.; Hume, S. P. *Quant. Funct. Brain Imaging PET* **1998**, 299.
- Haradahira, T.; Zhang, M. R.; Maeda, J.; Okauchi, T.; Kawabe, K.; Kida, T.; Suzuki, K.; Suhara, T. *Nucl. Med. Biol.* **2000**, *27*, 357.
- Haradahira, T.; Suhara, S.; Okauchi, T.; Maeda, J.; Arai, T.; Sasaki, S.; Yamamoto, F.; Maeda, M.; Suzuki, K. *World J. Nucl. Med.* **2002**, *1*, S183.
- Chapman, A. G.; Dürmüller, N.; Harrison, B. L.; Baron, B. M.; Parvez, N.; Meldrum, B. S. *Eur. J. Pharmacol.* **1995**, *274*, 83.
- Rowley, M.; Kulagowski, J. J.; Watt, A. P.; Rathbone, D.; Stevenson, G. I.; Carling, R. W.; Baker, R.; Marshall, G. R.; Kemp, J. A.; Foster, A. C.; Grimwood, S.; Hargreaves, R.; Hurley, C.; Saywell, K. L.; Tricklebank, M. D.; Leeson, P. D. *J. Med. Chem.* **1997**, *40*, 4053.
- Fuchigami, T.; Haradahira, T.; Fujimoto, N.; Okauchi, T.; Maeda, J.; Suzuki, K.; Suhara, T.; Yamamoto, F.; Sasaki, S.; Mukai, T.; Yamaguchi, H.; Ogawa, M.; Magata, Y.; Maeda, M. *Nucl. Med. Biol.* **2008**, *35*, 203.
- Kulagowski, J. J.; Baker, R.; Curtis, N. R.; Leeson, P. D.; Mawer, I. M.; Moseley, A. M.; Ridgill, M. P.; Rowley, M.; Stansfield, I.; Foster, A. C.; Geimwood, S.; Hill, R. G.; Kemp, J. A.; Marshall, G. R. *J. Med. Chem.* **1994**, *37*, 1402.
- Antilla, J. C.; Buchwald, S. L. *Org. Lett.* **2001**, *3*, 2077.
- Hans, A. U.S. Patent 5,633,379, 1995.
- Kulagowski, J. J.; Rowley, M.; Leeson, P. D.; Mawer, I. M. Eur. Patent 0,481,676, 1992.
- Danysz, W.; Kozela, E.; Parsons, C. G.; Sladek, M.; Bauer, T.; Popik, P. *Neuropharmacology* **2005**, *48*, 360.
- SPARC On Line Calculator: <http://sparc.chem.uga.edu/sparc/>.
- Haradahira, T.; Maeda, J.; Okauchi, T.; Zhang, M.-R.; Hojo, J.; Kida, T.; Arai, T.; Yamamoto, F.; Sasaki, S.; Maeda, M.; Suzuki, K.; Suhara, T. *Nucl. Med. Biol.* **2002**, *29*, 517.
- Pangalos, M. N.; Francis, P. T.; Foster, A. C.; Pearson, R. C. A.; Middlemen, D. N.; Bowen, D. M. *Brain Res.* **1992**, *596*, 223.
- Wamsley, J. K.; Sofia, R. D.; Faull, R. L. M.; Ary, T.; Narang, N.; McCabe, R. T. *Brain Res. Bull.* **1994**, *35*, 205.
- Kuryatov, A.; Laube, B.; Betz, H.; Kuhse, J. *Neuron* **1994**, *12*, 1291.
- Wafford, K. A.; Kathoria, M.; Bain, C. J.; Marshall, G.; Le Bourdellès, B.; Kemp, J. A.; Whiting, P. J. *Mol. Pharmacol.* **1995**, *47*, 374.
- O'Shea, R. D.; Manallack, D. T.; Conway, E. L.; Mercer, L. D.; Beart, P. M. *Exp. Brain Res.* **1991**, *86*, 652.
- Mugnaini, M.; Antolini, M.; Corsi, M.; van Amsterdam, F. J. *Recept. Signal Transduct. Res.* **1998**, *18*, 91.
- Dischino, D. D.; Welch, M. J.; Kilbourn, M. R.; Raichle, M. E. *J. Nucl. Med.* **1983**, *24*, 1030.
- Hashimoto, A.; Nishikawa, T.; Oka, T.; Takahashi, K. *J. Neurochem.* **1993**, *60*, 783.
- Haradahira, T.; Okauchi, T.; Maeda, J.; Zhang, M.-R.; Nishikawa, T.; Konno, R.; Suzuki, K.; Suhara, T. *Synapse* **2003**, *50*, 130.
- Nakagawa, S.; Deli, M. A.; Kawaguchi, H.; Shimizudani, T.; Shimonoto, T.; Kittel, A.; Tanaka, K.; Niwa, M. *Neurochem. Int.* **2009**, *54*, 253.
- Ishiwata, K.; Kawamura, K.; Yanai, K.; Hendrikse, N. H. *J. Nucl. Med.* **2007**, *48*, 81.
- Kikuchi, R.; Kusuhara, H.; Sugiyama, D.; Sugiyama, Y. *J. Pharmacol. Exp. Ther.* **2003**, *306*, 51.
- Wuest, F.; Kniess, T.; Henry, B.; Peeters, B. W.; Wiegerinck, P. H.; Pietzsch, J.; Bergmann, R. *Appl. Radiat. Isot.* **2009**, *67*, 308.
- Ogawa, K.; Mukai, T.; Kawai, K.; Takamura, N.; Hanaoka, H.; Hashimoto, K.; Shiba, K.; Mori, H.; Saji, H. *Eur. J. Nucl. Med. Mol. Imaging* **2009**, *36*, 115.
- Yamasaki, K.; Kuga, N.; Takamura, N.; Furuya, Y.; Hidaka, M.; Iwakiri, T.; Nishii, R.; Okumura, M.; Kodama, H.; Kawai, K.; Arimori, K. *Biol. Pharm. Bull.* **2005**, *28*, 549.